Inorganic Chemistry

Article

pubs.acs.org/IC

Cu^{II} and Cu^{I} Coordination Complexes Involving Two Tetrathiafulvalene-1,3-benzothiazole Hybrid Ligands and Their Radical Cation Salts

Sayo Yokota,[†] Keijiro Tsujimoto,[†] Sadayoshi Hayashi,[†] Fabrice Pointillart,[‡] Lahcène Ouahab,[‡] and Hideki Fujiwara*[,†]

[†]Department of Chemistry, Graduate School of Science, Osaka Prefecture University, 1-1 Gakuen-cho, Naka-ku, Sakai, Osaka 599-8531, Japan

[‡]Equipe Organométalliques: Matériaux et Catalyse, Institut des Sciences Chimiques de Rennes, UMR 6226, CNRS-Université de Rennes 1, Campus de Beaulieu, 35042 Rennes Cedex, France

Supporting Information

ABSTRACT: Preparations, crystal structure analyses, and magnetic property investigations on a new $Cu^{II}(hfac)_2$ complex coordinated with two TTF—CH═CH—BTA ligands, where hfac is hexafluoroacetylacetonate, TTF is tetrathiafulvalene, and BTA is 1,3-benzothiazole, are reported together with those of its dicationic AsF_6^- salt, $[Cu(hfac)_2(TTF—CH═CH—BTA)_2](AsF_6)_2$, in which each TTF part is in a radical cation state. In these $Cu^{II}(hfac)_2$ complexes, two ligands are bonded to the central Cu atom of the $Cu(hfac)_2$ part through the nitrogen atom of the 1,3-benzothiazole ring and occupy the two apical positions of the $Cu(hfac)_2$ complex with an elongated octahedral geometry. These two ligands are located parallelly in a transverse head-to-tail manner, and the $Cu(hfac)_2$ moiety is closely sandwiched by these two ligands. In the AsF_6^- salt of the $Cu(hfac)_2$ complex, each TTF dimer is separated by the AsF_6^- anions and has no overlap with each other within the one-dimensional arrays, resulting in an insulating behavior. Both $Cu(hfac)_2$ complexes showed the simple Curie-like temperature dependence of paramagnetic susceptibilities (χ_M), indicating that no interaction exists between the paramagnetic Cu^{II} d spins. Furthermore, crystal structure analysis and magnetic/conducting properties of a radical cation ReO_4^- salt of the Cu^{I} complex with two TTF—CH═CH—BTA ligands, $[Cu(TTF—CH═CH—BTA)_2](ReO_4)_2$, are also described. Two nitrogen atoms of the ligands are connected to the central Cu^{I} in a linear dicoordination with a Cu—N bond length of 1.879(9) Å. Two TTF parts of the neighboring complexes form a dimerized structure, and such a TTF dimer forms a one-dimensional uniform array along the *a* direction with a short S—S contact of 3.88 Å. Magnetic property measurement suggested the existence of a strongly antiferromagnetic one-dimensional uniform chain of $S = 1/2$ spins that originate from the radical cation states of the TTF dimers. Due to the construction of the one-dimensional uniform array of the radical cation state of the TTF dimer along the *a* axis, a semiconducting behavior is observed with σ_{rt} = of 6×10^{-5} S cm^{-1} and an activation energy of E_a = 0.16 eV.

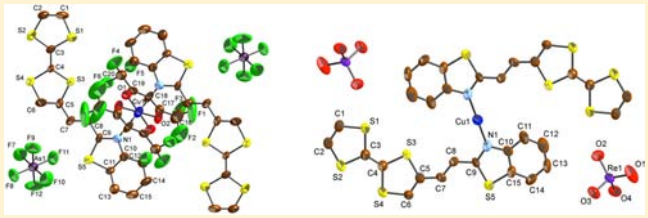

1. INTRODUCTION

Development of photofunctional materials using donor—acceptor (D—A) type dyads based on TTF frameworks, where TTF is tetrathiafulvalene, has been intensively studied for application to organic materials such as fluorescence switches, metal ion sensors, photovoltaic cells, and nonlinear optics.[1−7] We developed several D—A dyads using the TTF framework and fluorescent molecules such as 2,5-diphenyl-1,3,4-oxadiazole (PPD) and fluorene and reported their crystal structures and electrochemical and optical properties.[8−11] Among them, a new D—A dyad, TTF—CH═CH—BTA, **1**, in which a 1,3-benzothiazole (BTA) ring is connected with the TTF part through an ethylene spacer, was synthesized to realize photoswitchable conductors and photoelectric conversion materials.[12] A single-crystalline sample of **1** showed generation of photocurrents along the segregated stackings of the TTF and BTA parts by a photoinduced intramolecular electron transfer and resultant formation of a charge-separated state.

On the other hand, development of magnetic-conducting bifunctional materials has been also intensively studied.[13−18] The π—d interactions between conducting π electrons and magnetic d spins on transition metal centers such as Fe^{III} have played important roles to produce peculiar physical phenomena such as magnetic-field-induced superconductivities in λ-$(BETS)_2FeCl_4$ and κ-$(BETS)_2FeBr_4$ salts.[19,20] Among them, novel π—d complexes based on the D—A-type TTF derivatives containing heteroaromatic rings such as pyridine, pyrazine, and oxazoline rings have been also prepared because nitrogen atoms in such heteroaromatic rings can coordinate to the magnetic

Received: February 28, 2013
Published: May 16, 2013

   dx.doi.org/10.1021/ic4005246 | *Inorg. Chem.* 2013, 52, 6543−6550

Chart 1. Molecular Structures of Ligand 1 and Its Copper Complexes, $Cu(hfac)_2(1)_2$ and $Cu(1)_2$

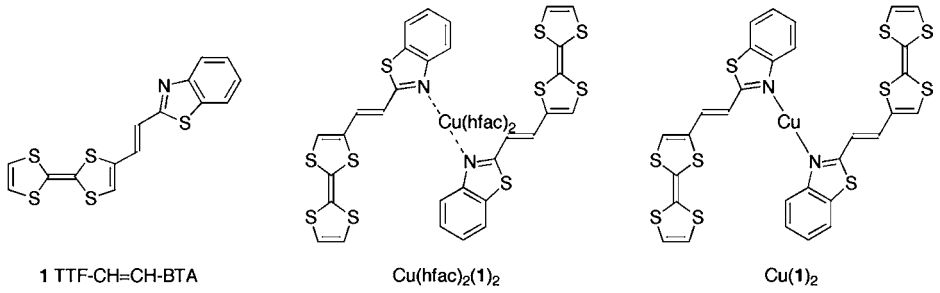

Scheme 1. Synthesis of Ligand 1

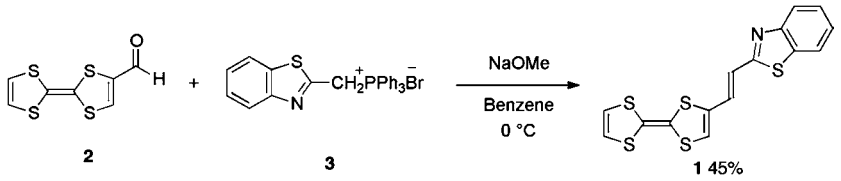

Table 1. Crystal Data and Structure Refinement Details

	$Cu(hfac)_2(1)_2$	$[Cu(hfac)_2(1)_2](AsF_6)_2$	$[Cu(1)_2](ReO_4)_2$
cryst habit	brown plate	black plate	black block
chem formula	$C_{20}H_{10}Cu_{0.50}F_6NO_2S_5$	$C_{20}H_{10}AsCu_{0.50}F_{12}NO_2S_5$	$C_{15}H_9Cu_{0.50}NO_4ReS_5$
M (g mol^{-1})	602.37	791.28	645.52
cryst syst	monoclinic	triclinic	triclinic
space group	$P2_1/a$	$P\bar{1}$	$P\bar{1}$
a (Å)	9.347(4)	9.7572(10)	8.688(5)
b (Å)	18.490(8)	11.2053(11)	10.553(5)
c (Å)	14.046(6)	14.0561(14)	10.917(6)
α (deg)	90	65.509(2)	74.207(16)
β (deg)	102.817(8)	78.065(3)	87.89(2)
γ (deg)	90	78.086(3)	73.922(15)
V (Å^3)	2366.9(18)	1355.7(2)	924.7(9)
Z	4	2	2
D_{calcd} (g cm^{-3})	1.690	1.938	2.318
μ(Mo Kα) (cm^{-1})	9.93	21.26	77.2
F(000)	1206	777	615
no. of reflns collcd	21 307	13 316	8163
no. of indep reflns	6727	6130	4899
no. of obsd reflns [$I > 2\sigma(I)$]	1909	2722	3524
R_{int}	0.077	0.121	0.034
no. of params refined	323	386	250
R_1	0.058	0.053	0.066
wR_2	0.040	0.128	0.068
S	1.220	1.063	1.100
$\Delta\rho_{min}$ (e Å^{-3})	0.39	0.94	1.61
$\Delta\rho_{max}$ (e Å^{-3})	−0.36	−0.93	−2.06

transition metal atoms like as Mn^{II}, Co^{II}, Ni^{II}, and Cu^{II},[21−27] and new kinds of π−d systems having magnetic-conducting bifunctionalities have been yielded through direct coordination to magnetic transition metal centers. From this point of view, we tried to apply the hybrid molecule **1** as a coordination ligand to transition metal complexes and focused on $M(hfac)_2$ (M = Mn^{II}, Co^{II}, Ni^{II}, Cu^{II}, etc., hfac = hexafluoroacetylacetonate) complexes because the $M(hfac)_2$ complexes have been often used as key building blocks for construction of novel magnetic materials.[28−31]

In this paper, we reported the preparation, crystal structure analyses, and magnetic properties of the neutral $Cu(hfac)_2$ complex coordinated with two TTF—CH═CH—BTA ligands **1**, $Cu(hfac)_2(1)_2$, and its dicationic AsF_6^- salt, $[Cu(hfac)_2(1)_2](AsF_6)_2$, Chart 1. Furthermore, we also describe the preparation and structure analysis of the radical cation ReO_4^- salt of an unprecedented Cu^I complex with two TTF—CH═CH—BTA ligands **1**, $[Cu(1)_2](ReO_4)_2$. Investigations on its magnetic and conducting properties are also discussed.

2. EXPERIMENTAL SECTION

Synthesis of 1. Ligand **1** was synthesized according to our previous procedure, Scheme 1.[12] Thus, Wittig reagent **3** was prepared from 2-methyl-1,3-benzothiazole according to the reported meth-

dx.doi.org/10.1021/ic4005246 | Inorg. Chem. 2013, 52, 6543−6550

ods.[32,33] Then, compound **3** (123 mg. 0.25 mmol) was reacted successively with 28 wt % NaOMe in methanol (0.75 mmol) and formyl-TTF **2**[34] (58 mg, 0.25 mmol) in benzene (30 mL) at 0 °C. After stirring overnight, the solution was evaporated in vacuo and the residue was separated by a column-chromatography on silica gel with $CHCl_3$/*n*-hexane (2:1, v/v) as an eluent. After recrystallization from $CHCl_3$/*n*-hexane, ligand **1** (41 mg) was obtained as a reddish-purple powder in 45% yield. ^{1}H NMR coupling constants ($J \approx 15$ Hz) of the ethylene spacer part of **1** suggested that the ethylene spacer has only a trans configuration. Mp 153−156 °C (dec.). ^{1}H NMR (300 MHz, acetone-d_6): δ 8.01 (d, J = 7.8 Hz, 1H), 7.94 (d, J = 7.8 Hz, 1H), 7.58 (d, J = 15.3 Hz, 1H), 7.51 (dd, J = 7.8 Hz, J = 7.8 Hz, 1H), 7.42 (dd, J = 7.8 Hz, J = 7.8 Hz, 1H), 7.22 (s, 1H), 6.67 (s, 2H), 6.67 (d, J = 15.3 Hz, 1H). HRMS FAB$^+$ (matrix 3-nitrobenzyl alcohol) ($C_{15}H_9S_5N$): calcd, 362.9339; found, 362.9307. IR (KBr) ν (cm^{-1}): 646, 751, 951, 988, 1099, 1428, 1473, 1599, 3051.

Preparation of Cu(hfac)$_2$(1)$_2$ Complex. To a stirred solution of $Cu(hfac)_2{\cdot}2H_2O$ (4.7 mg, 0.01 mmol) in boiling cyclohexane (20 mL) was added ligand **1** (7.3 mg, 0.02 mmol). Then the mixture was further refluxed for 10 min and slowly cooled to room temperature. The reaction mixture was slowly added with *n*-hexane and kept at 16 °C for several days. The neutral $Cu(hfac)_2$ complex coordinated with two hybrid ligands **1**, $Cu(hfac)_2(\mathbf{1})_2$, was obtained as brown platelet crystals.

Preparation of Radical Cation Salts Based on the Cu(hfac)$_2$ Complex of Ligand 1. Preparations of radical cation salts were performed by an electrochemical oxidation method. The AsF_6^- salt based on the $Cu(hfac)_2$ complex of ligand **1**, $[Cu(hfac)_2(\mathbf{1})_2](AsF_6)_2$, was prepared as black platelet crystals by a galvanostatic (I = 1.0 μA) oxidation of TTF—CH═CH—BTA **1** (10 mg) in the presence of $Cu(hfac)_2{\cdot}2H_2O$ (14 mg) and *n*-$Bu_4N{\cdot}AsF_6$ (200 mg) as a supporting electrolyte under a nitrogen atmosphere in the mixture of dry CH_2Cl_2 and dry cyclohexane (20 mL, v/v = 3:4) at 16 °C for several days. On the other hand, the ReO_4^- salt, $[Cu(\mathbf{1})_2](ReO_4)_2$, was prepared as black block-like crystals by a galvanostatic (I = 0.5 μA) oxidation of **1** (4 mg) in the presence of $Cu(hfac)_2{\cdot}2H_2O$ (14 mg) and *n*-$Bu_4N{\cdot}ReO_4$ (200 mg) under a nitrogen atmosphere in the mixture of dry chlorobenzene and ethanol (16 mL, v/v = 9:1) at 40 °C for several days. The chemical compositions of these obtained radical cation salts were determined by X-ray crystal structure analyses.

X-ray Data Collection, Structure Solution, and Refinement. X-ray diffraction data were collected at 293 K for single crystals of $Cu(hfac)_2(\mathbf{1})_2$ and $[Cu(\mathbf{1})_2](ReO_4)_2$ on a Rigaku AFC-7 Mercury CCD diffractometer with graphite-monochromated Mo Kα radiation (λ = 0.71070 Å) and for the single crystal of $[Cu(hfac)_2(\mathbf{1})_2](AsF_6)_2$ on a Rigaku RAXIS-RAPID imaging plate diffractometer with a graphite-monochromated Mo Kα radiation (λ = 0.71070 Å). Structures of these compounds were solved by a direct method (SIR92),[35] expanded by DIRDIF94,[36] and refined on F^2 with a full-matrix least-squares analysis. Calculated positions of hydrogen atoms [d(C−H) = 0.95 Å] were included but not refined in the final calculations. All calculations were performed using the CrystalStructure crystallographic software package from Molecular Structure Corp.[37] Crystal data and structure refinement parameters are given in Table 1 and selected bond lengths in Table 2.

Electrical Conductivity, SQUID, and EPR Measurements. Electrical conductivities were measured on a single crystal of $[Cu(\mathbf{1})_2](ReO_4)_2$ in the temperature range from 120 to 300 K by the two-terminal method. Two gold electrodes (15 $\mu\phi$) were contacted to a single crystal with a gold paste parallel to the a axis. Magnetizations were measured in the temperatures range from 1.9 to 300 K under an applied field of 5.0 kOe with a SQUID magnetometer (MPMS-XL, Quantum Design). Paramagnetic susceptibilities (χ_M) were obtained by subtracting the diamagnetic contribution estimated using Pascal's constants[38] from the observed magnetic susceptibilities. EPR spectra of powder samples of $Cu(hfac)_2(\mathbf{1})_2$ and $[Cu(\mathbf{1})_2](ReO_4)_2$ were measured at room temperature with a JEOL JES-RE1X X-band ESR spectrometer.

Table 2. Selected Bond Lengths (Angstroms) and Estimation of the Charge Q on the TTF Moieties

	$Cu(hfac)_2(\mathbf{1})_2$	$[Cu(hfac)_2(\mathbf{1})_2](AsF_6)_2$	$[Cu(\mathbf{1})_2](ReO_4)_2$
Cu−N1	2.493(4)	2.559(9)	1.879(9)
Cu−O1	1.958(3)	1.945(7)	
Cu−O2	1.936(3)	1.937(12)	
C═C (a)[a]	1.31(1)	1.38(1)	1.35(1)
C−S (b)[a]	1.76	1.72	1.74
C−S (c)[a]	1.72	1.72	1.73
C═C (d)[a]	1.32	1.34	1.34
$\delta = (b + c) - (a + d)$	0.85	0.72	0.78
Charge Q[b]	+0.003	+0.97	+0.53

[a]Averaged values of the corresponding C−S (b, c) and C═C (a, d) bonds.

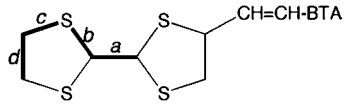

[b]Charge Q was estimated by the equation $Q = 6.347 - 7.463\delta$ (ref 35).

3. RESULTS AND DISCUSSION

3.1. Crystal Structure and Magnetic Properties of Cu(hfac)$_2$(1)$_2$. X-ray crystal structure analysis of the neutral $Cu(hfac)_2$ complex of ligand **1** was performed at room temperature. The crystal belongs to the monoclinic space group $P2_1/a$. In the unit cell, one ligand **1** and one-half of the $Cu(hfac)_2$ unit are crystallographically independent and the Cu atom is located on the inversion center, suggesting the formula of this complex to be $Cu(hfac)_2(\mathbf{1})_2$. The molecular structure of the $Cu(hfac)_2(\mathbf{1})_2$ complex is shown in Figure 1. Bond lengths of the TTF—CH═CH—BTA ligand moiety are close to those for the noncoordinated neutral ligand unit **1**,[12] indicating that both $Cu(hfac)_2$ part and ligands **1** are in the neutral valence state. Two ligands **1** are bonded to the central Cu atom of the $Cu(hfac)_2$ part with a bond length of 2.49 Å through the nitrogen atom of the 1,3-benzothiazole ring and occupy the two apical positions of the $Cu(hfac)_2$ complex with an elongated octahedral geometry. This Cu−N bond length is relatively longer than that of the reported $Cu(hfac)_2$(TTF—CH═CH—py)$_2$ (py = 4-pyridine) (2.031(7) Å) and $Cu(hfac)_2$(TTF—CH═N—pyz)$_2$ (2.053(2) Å) (pyz = 2-pyrazine) complexes,[21,22] suggesting its weaker through-bond metal−ligand interaction. The increase of the Cu−N bond length is due to the orientation of the Jahn−Teller axis along the N−Cu−N axis in $Cu(hfac)_2(\mathbf{1})_2$, while it is in the plane formed by the $hfac^-$ anions in the previously published complexes. The TTF and $Cu(hfac)_2$ parts are almost orthogonal with a dihedral angle of 74.6°. The two ligands **1** are located parallelly in a transverse head-to-tail manner, and the $Cu(hfac)_2$ moiety is closely sandwiched by these two ligands, suggesting its preferable coordination structure to realize strong π−d interactions. Such a structural feature is different from those reported in $Cu(hfac)_2$(TTF—CH═CH—py)$_2$[21] and $Cu(hfac)_2$(DMT-TTF—py)$_2$[23] complexes in which the TTF parts of the complexes are very far from the $Cu(hfac)_2$ part through para coordination of the pyridine parts. On the other hand, the $Cu(hfac)_2$(1,3-benzothiazole)$_2$ parts and the TTF parts form a segregated layer structure along the b axis in the crystal as shown in Figure 2. Each TTF core is overlapped with the TTF core of the neighboring column, and they form a strongly

dx.doi.org/10.1021/ic4005246 | Inorg. Chem. 2013, 52, 6543−6550

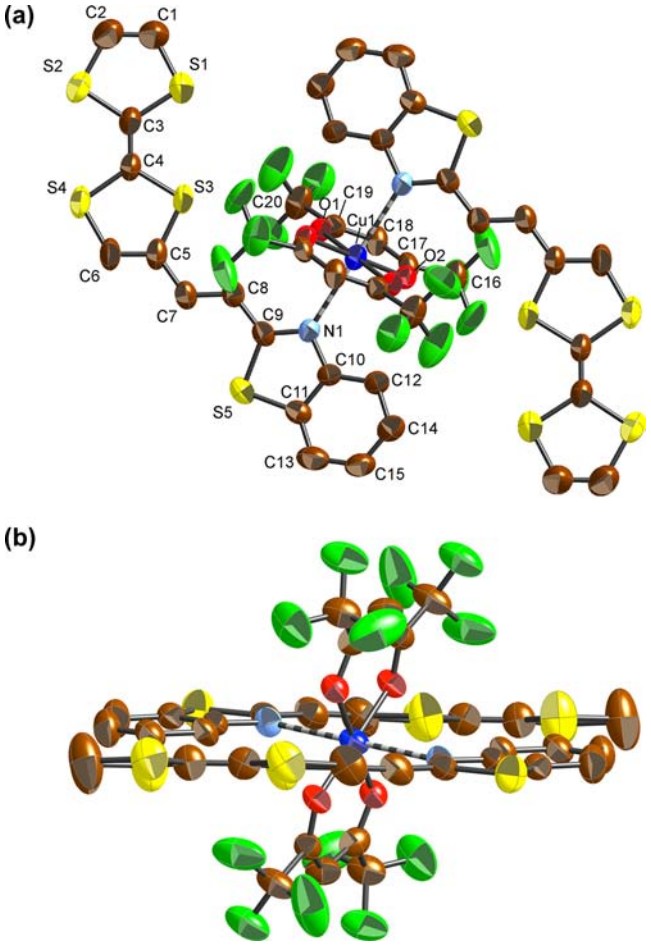

Figure 1. ORTEP drawings (ellipsoids at 50% probability level) of the molecular structures of the $Cu(hfac)_2(\mathbf{1})_2$ complex. (a) Top view and (b) side view of the complex. Hydrogen atoms omitted for clarity.

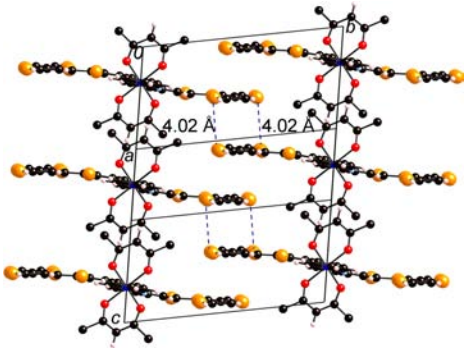

Figure 2. Crystal structure of the $Cu(hfac)_2(\mathbf{1})_2$ complex. Fluorine atoms omitted for clarity.

dimerized structure with an interplanar distance of 3.74 Å (the shortest S−S contact is 4.02 Å). However, there is no overlap between adjacent TTF dimers, suggesting a weak intracolumnar interaction. Insulating behavior is observed because this complex is in the neutral state, and there is no favorable conducting pathway between the TTF units.

Molar paramagnetic susceptibilities (χ_M) of the polycrystalline sample of the $Cu(hfac)_2(\mathbf{1})_2$ complex were measured at 5.0 kOe in the temperature range of 1.9−300K. The temperature dependence of χ_M values of the $Cu(hfac)_2(\mathbf{1})_2$ complex completely obeys the simple Curie law ($\chi_M = C/T$) with a Curie constant (C) of 0.452 emu K mol^{-1}, indicating that no interaction exists between the paramagnetic Cu^{II} d spins (S = 1/2, g = 2.19) (see Figure S1, Supporting Information). The EPR spectrum of the powder sample of $Cu(hfac)_2(\mathbf{1})_2$ was measured at room temperature. The EPR spectrum shows typical signals for Cu^{II} species having an elongated octahedral geometry with anisotopic g values of $g_{\|}$= 2.36 and $g_{\perp}$ = 2.08 and a hyperfine structure (coupling constant $A_{\|}$ of 12 mT (56×10^{-4} cm^{-1})) (see Figure S3, Supporting Information). Thus, the average g value of 2.17 is in agreement with magnetic susceptibility measurements. These results suggest that the orbital ground state is the d_{x2-y2} orbital, and the two axial benzothiazole ligands coordinate to the Cu^{II} d-spin center very weakly.

3.2. Preparation, Crystal Structures, and Physical Properties of Radical Cation Salts. For realization of good conducting properties, generation of conducting carriers in the columns of donor molecules is one of the indispensable factors as observed in conventional organic conductors. Therefore, we attempted to obtain radical cation salts based on the $Cu(hfac)_2$ complex of hybrid ligand **1** by an electrochemical oxidation method, and we obtained two kinds of dicationic salts, $[Cu(hfac)_2(\mathbf{1})_2](AsF_6)_2$ as black platelet crystals and $[Cu(\mathbf{1})_2](ReO_4)_2$ as black block-like crystals, by galvanostatic oxidation of **1** in the presence of $Cu(hfac)_2{\cdot}2H_2O$ and the corresponding tetra-*n*-butylammonium salts of these anions. These chemical compositions of the obtained salts were determined by X-ray crystal structure analyses as discussed below.

3.2.1. Crystal Structure and Magnetic Properties of $[Cu(hfac)_2(1)_2](AsF_6)_2$. X-ray crystal structure analysis of the AsF_6^- salt based on the $Cu(hfac)_2(\mathbf{1})_2$ complex was performed at room temperature. The space group of the AsF_6^- salt is triclinic $P\bar{1}$, and the unit cell contains one $Cu(hfac)_2(\mathbf{1})_2$ unit and two AsF_6^- anions, suggesting the formula of the salt to be $[Cu(hfac)_2(\mathbf{1})_2]^{2+}(AsF_6^-)_2$. The molecular structure of the AsF_6^- salt is shown in Figure 3. The ligands occupy the apical positions, and they are trans to each other and bonded to the Cu atom with a Cu−N bond length of 2.56 Å, which is a little longer than the neutral $Cu(hfac)_2(\mathbf{1})_2$ complex. This observation is due to oxidation of the TTF-based ligand, leading to a decrease of the Lewis base character. The central C═C bond length value of the TTF moiety is 1.385(15) Å and longer than that found in the neutral complex (1.315(11) Å), suggesting the positively charged state of the TTF part. Using the averaged C−S (b, c) and C═C (a, d) bond lengths of the TTF moiety, the charge Q on the TTF moiety can be estimated by the equation $Q = 6.347 - 7.463\,\delta$, where $\delta = (b + c) - (a + d)$, proposed by Guionneau et al. (see Table 2).[39] The calculated Q value of this AsF_6^- salt is +0.97 and suggests the radical monocation state of the TTF moiety. Thus, the following charge distribution might be deduced as $[Cu^{2+}(hfac^-)_2(\mathbf{1}^{\bullet+})_2](AsF_6^-)_2$. TTF and $Cu(hfac)_2$ moieties form a dihedral angle of 114.8°. This dihedral angle is larger than that in the neutral complex (74.6°), suggesting that the $hfac^-$ ligands are tilted toward the 1,3-benzothiazole part in comparison to the neutral complex. As shown in Figure 4, two TTF parts of the neighboring complexes form a strongly dimerized structure with an interplanar distance of 3.37 Å and the shortest S−S contact of 3.43 Å, which is much shorter than the sum of van der Waals radii (3.60 Å). As a result, there is a one-dimensional array of (TTF dimer)−($Cu(hfac)_2$)−(TTF dimer)− along the [1 0 −1] direction. However, each TTF dimer is separated by the AsF_6^- anions and has no overlap with

dx.doi.org/10.1021/ic4005246 | Inorg. Chem. 2013, 52, 6543−6550

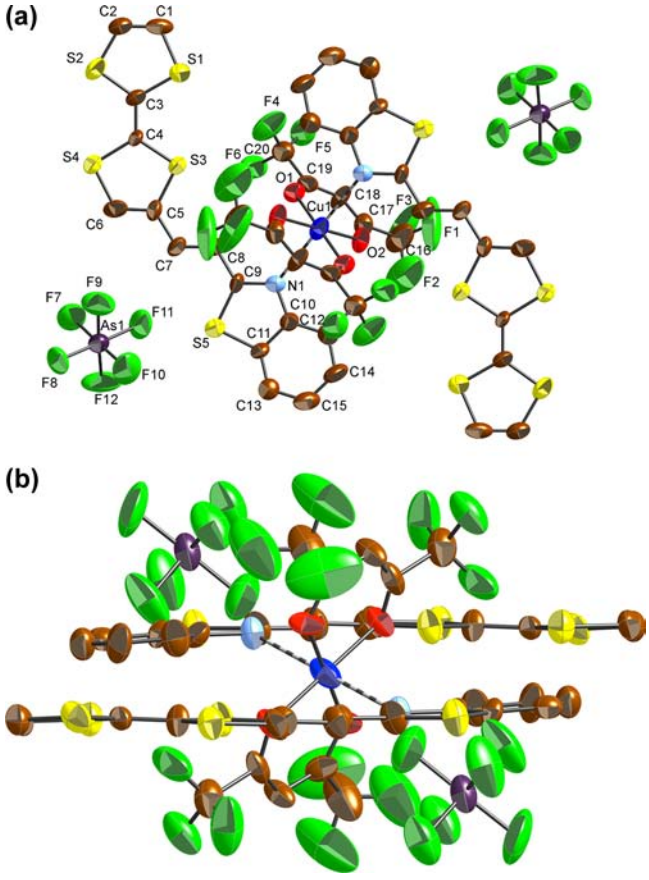

Figure 3. ORTEP drawings (ellipsoids at 50% probability level) of the molecular structure of the $[Cu(hfac)_2(\mathbf{1})_2](AsF_6)_2$ salt. (a) Top view and (b) side view of the AsF_6^- salt. Hydrogen atoms omitted for clarity.

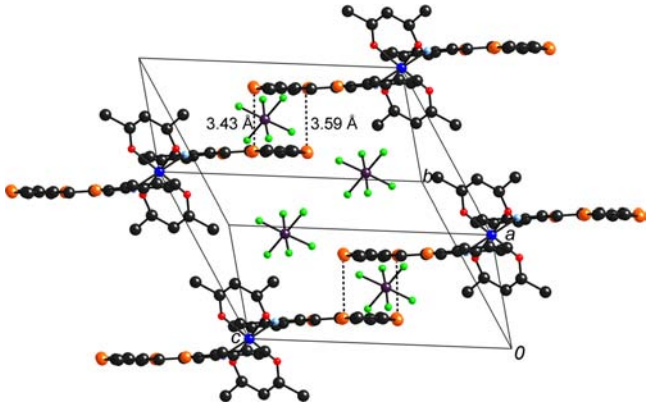

Figure 4. Crystal structure of the $[Cu(hfac)_2(\mathbf{1})_2](AsF_6)_2$ salt. Hydrogen and fluorine atoms omitted for clarity.

each other within the one-dimensional array. The adjacent TTF dimers largely shift along the *a* axis with a value of 7.10 Å, indicating that no preferable conducting pathway exists in the crystal structure. The shortest S−S contact between the TTF parts is 3.43 Å, which is short enough to expect a good conducting behavior; however, the AsF_6^- anion molecule is located between the dimers to break in the conductive pathway. Therefore, the AsF_6^- salt is cleared to be an insulator.

Molar paramagnetic susceptibilities (χ_M) of the polycrystalline sample of $[Cu(hfac)_2(\mathbf{1})_2](AsF_6)_2$ were measured at 5.0 kOe in the temperature range of 1.9−300 K. They obey the simple Curie-like temperature dependence with a Curie constant (C) of 0.443 emu K mol^{-1} (S = 1/2, g = 2.17), also suggesting the isolated nature of the Cu^{II} d spins as observed in the neutral complex (see Figure S2, Supporting Information). Because no contribution from the radical cation state of the TTF—CH═CH—BTA part was observed, two TTF radical cation spins in one TTF dimer are considered to be strongly dimerized in the singlet spin state (antiferromagnetically coupled) as expected from crystal structure analysis of the salt.

3.2.2. Crystal Structure and Physical Properties of [Cu(1)$_2$](ReO$_4$)$_2$. X-ray crystal structure analysis of a black platelet crystal of the ReO_4^- salt was performed at room temperature. The space group of the ReO_4^- salt is triclinic $P\bar{1}$ and there is one ligand **1**, one ReO_4^- anion, and a Cu atom located on the center of inversion symmetry as a crystallographically independent unit, suggesting the formula of the salt to be $[Cu(\mathbf{1})_2](ReO_4)_2$. Despite the use of $Cu(hfac)_2{\cdot}2H_2O$ compound during electrochemical oxidation, $hfac^-$ ligands are eliminated from the copper center and are not included in the obtained salt. The molecular structure of this ReO_4^- salt is shown in Figure 5. Two nitrogen atoms of ligand **1** are connected to the central copper atom in a linear dicoordination with a much shorter Cu−N bond length of 1.879(9) Å than those of the other $Cu(hfac)_2(\mathbf{1})_2$ complexes. Because such a linear dicoordination was often observed in Cu^I complexes, the valence of the central copper atom seems to be +1. Ligand **1** has a highly planar structure with the largest deviation of 0.16 Å from the molecular least-squares plane. Figure 6 shows the crystal structure projected down to the *bc* plane. ReO_4^- anions locate on the top and bottom of the central copper atom, and four oxygen atoms of two ReO_4^- anions have short contacts of Cu−O(1) = 2.867(10) Å and Cu−O(3) = 2.898(12) Å with the central copper atom, suggesting that the ReO_4^- anions are not coordinated but weakly interacted with the central copper atom. Each complex is located around the center of symmetry, and two TTF parts of the neighboring complexes in the [1 −1 1] direction form a dimerized structure with short S−S contacts of 3.52 and 3.69 Å. Furthermore, there is a comparatively short S−S contact of 3.88 Å between the TTF moieties of the adjacent ligands along the *a* axis, resulting in formation of a one-dimensional uniform array of TTF dimers along the *a* direction as shown in Figure 7. Therefore, construction of the one-dimensional uniform conduction pathways along the *a* axis is achieved in this salt, and this is a quite different situation from the cases of the former insulating $Cu(hfac)_2(\mathbf{1})_2$ complex and $[Cu(hfac)_2(\mathbf{1})_2](AsF_6)_2$ salt. Overlap integrals between the neighboring TTF moieties were calculated on the basis of the extended Hückel approximation. The overlap integral in the dimer has a very large value of 23.5×10^{-3}, and a small value of 1.95×10^{-3} is calculated between the TTF moieties along the adjacent dimers, suggesting that a uniform side-by-side interaction between the dimers exists along the *a* axis.

Molar paramagnetic susceptibilities (χ_M) of the polycrystalline sample of the ReO_4^- salt were measured at 5.0 kOe to clear the charge distribution in this salt having the $[Cu(\mathbf{1})_2](ReO_4)_2$ composition because there are two possibilities of the valence state of the central copper atom (Cu^I or Cu^{II}). The temperature dependence of χ_M is shown in Figure 8 and fitted by a Bonner−Fisher's equation for the S = 1/2 spin chain system,[40] $[\chi_M = (N_A g^2 \mu_B{}^2/k_B T)(0.25 + 0.074975x + 0.075235x^2)/(1.0 + 0.9931x + 0.172135x^2 + 0.757825x^3)$, where $x = |J|/k_B T]$. The estimated magnetic exchange interaction J between S = 1/

dx.doi.org/10.1021/ic4005246 | Inorg. Chem. 2013, 52, 6543−6550

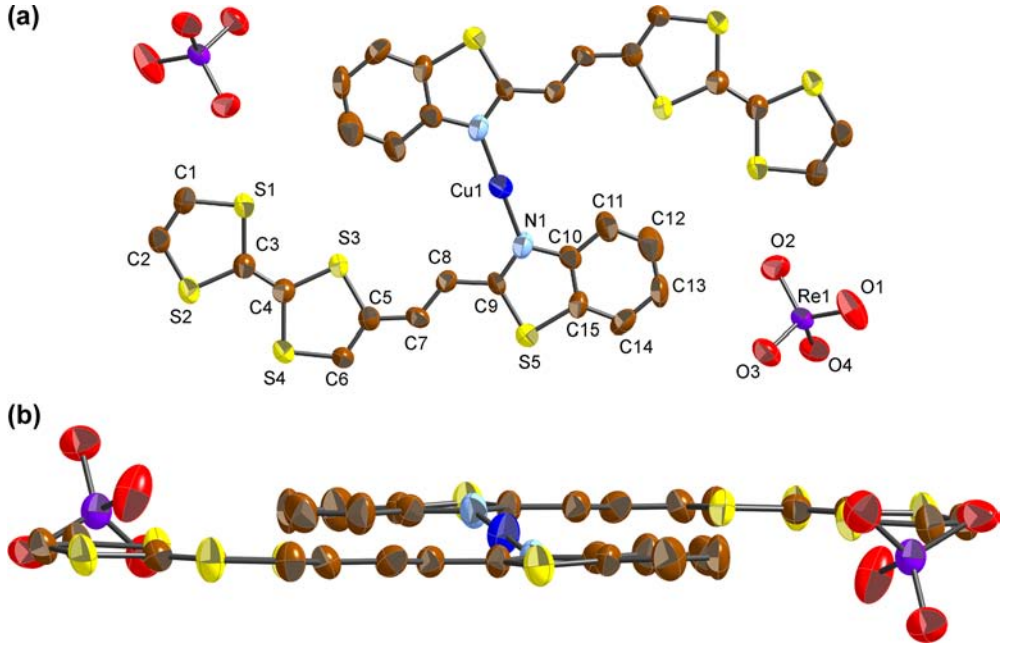

Figure 5. ORTEP drawings (ellipsoids at 50% probability level) of the molecular structure of the $[Cu(\mathbf{1})_2](ReO_4)_2$ salt. (a) Top view and (b) side view of the ReO_4^- salt. Hydrogen atoms omitted for clarity.

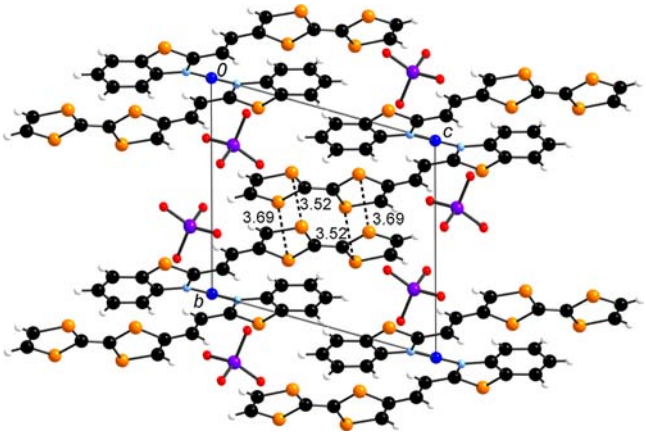

Figure 6. Crystal structure of the $[Cu(\mathbf{1})_2](ReO_4)_2$ salt projected onto the *bc* plane.

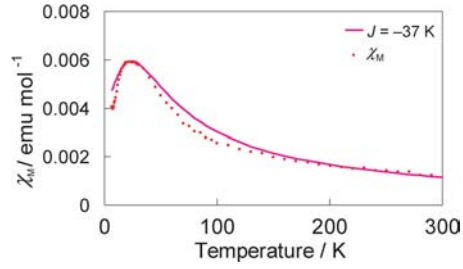

Figure 8. Temperature dependence of magnetic susceptibilities (χ_M) of the $[Cu(\mathbf{1})_2](ReO_4)_2$ salt. Solid line indicated the fitting curve of the Bonner−Fisher's equation for the $S = 1/2$ spin system with an antiferromagnetic exchange interaction of $J = -37$ K.

2 spins is $J = -37$ K and suggested the existence of a strongly antiferromagnetic one-dimensional uniform chain of $S = 1/2$ spins. Because each copper atom locates on the center of symmetry and is apart far from each other, magnetic $S = 1/2$ Cu^{II} species cannot be the origin of the magnetic properties of this salt. On the other hand, if we assumed that the copper atom is in the nonmagnetic Cu^{I} valence state, the charge distribution of the ReO_4^- salt can be determined to be

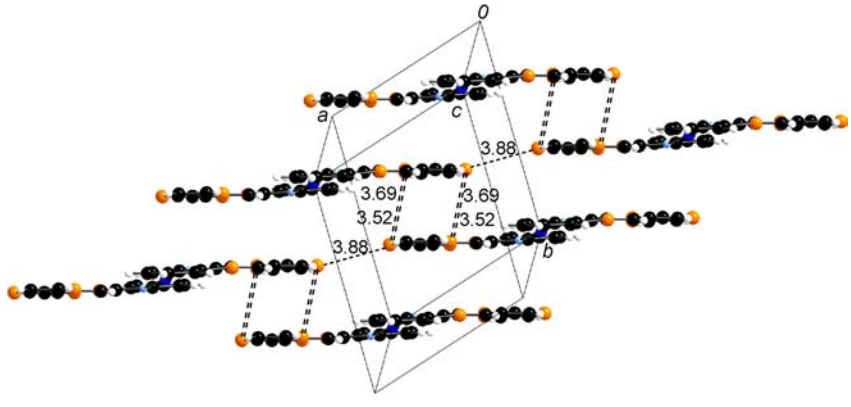

Figure 7. Array structure of the $[Cu(\mathbf{1})_2]^{2+}$ species along the *a* plane.

dx.doi.org/10.1021/ic4005246 | *Inorg. Chem.* 2013, 52, 6543−6550

$[Cu^{+}(\mathbf{1})_2^{+}](ReO_4^{-})_2$ and each dimer of ligand **1** has a +1 valence state and one $S = 1/2$ spin. The resultant charge Q of +0.5 on each TTF moiety is also assisted by the estimated Q value of +0.53 from the averaged C−S and C═C bond lengths of the TTF moiety (see Table 2).[39] Because the ligand dimers construct one-dimensional uniform arrays of the TTF moieties along the *a* direction with a relatively short S−S contact of 3.88 Å as mentioned before, the origin of the $S = 1/2$ spin chain is cleared to be the radical cation state of the TTF dimer, and this charge distribution $[Cu^{+}(\mathbf{1})_2^{+}](ReO_4^{-})_2$ is assumed. The EPR spectrum of the powder sample of $[Cu(\mathbf{1})_2](ReO_4)_2$ at room temperature showed typical signals for the TTF-based radical cation π spin with anisotopic g values of $g_x = 2.011$, $g_y = 2.007$, and $g_z = 2.002$ (see Figure S4, Supporting Information), clearly suggesting that the origin of the spin is the radical cation state of the TTF dimer.

Regaring the electronic structure of the dicationic $[Cu(\mathbf{1})_2]^{2+}$ part, we examined its molecular orbital calculation on the basis of the B3LYP DFT method using the LANL2DZ basis set for the copper atom and the 6-31G(d,p) basis set for the other atoms using the Gaussian09 package (see Figure S5, Supporting Information).[41] This calculation suggested that (1) the SOMO orbital localizes on both TTF moieties, (2) the central copper atom has +0.6 atomic charge and the other positive charges are distributed on all the sulfur atoms, namely, on the TTF moieties, and (3) spin densities localize on both TTF moieties. These results are in good agreement with the experimental results and suggest that the charge distribution of $[Cu^{+}(\mathbf{1})_2^{+}]$ is a stable electronic structure in the dicationic species $[Cu(\mathbf{1})_2]^{2+}$. As compared to the neutral $[Cu(hfac)_2(\mathbf{1})_2]$ complex, the $[Cu(\mathbf{1})_2]^{2+}$ part of $[Cu(\mathbf{1})_2](ReO_4)_2$ lacks two negatively charged $hfac^{-}$ ligands and is weakly interacted with two ReO_4^{-} anions. This replacement of the $hfac^{-}$ ligands to the ReO_4^{-} moieties may occur during electrochemical oxidation in the presence of the ReO_4^{-} anions, and the intramolecular charge reallocation from $[Cu^{2+}(\mathbf{1})_2]$ to $[Cu^{+}(\mathbf{1})_2^{+}]$ occurs due to the decrease of the negative charge around the central copper atom that originates from weak interactions with the ReO_4^{-} anions. In the case of the former AsF_6^{-} salt, such a ligand replacement did not occur due to the difference of chemical species and shape of the anion molecule (AsF_6^{-} vs ReO_4^{-}) and formation of $[Cu(\mathbf{1})_2](AsF_6)_2$ salt could not be realized. Such a charge reallocation between the TTF moiety and the Cu^{II} species was also observed in the coordination complexes (pyra-TTF)$_2$[Cu_3Cl_4(pyra-TTF)], where pyra-TTF is pyrazino-TTF, and $CuCl_{1.5}$(pyra-STF), where pyra-STF is pyrazinodiselenadithiafulvalene, in which reaction between the neutral pyra-TTF(STF) and $TBA_2Cu^{II}Cl_4$ yielded the charge transfer complexes, $(pyra\text{-}TTF)_2{}^{+}Cu^{I}{}_3Cl_4$ and $(pyra\text{-}STF)^{+0.5}Cu^{I}Cl_{1.5}$.[42,43] In particular, the $CuCl_{1.5}$(pyra-STF) salt afforded a high conductivity of 25 S cm^{-1} due to construction of pseudo-1D donor-ligand columns.

According to this charge distribution of $[Cu^{+}(\mathbf{1})_2^{+}](ReO_4^{-})_2$, each TTF moiety in the ligand dimer has a partially oxidized state of +0.5 and the one-dimensional array of the ligand dimers along the *a* axis may be conductive to some extent. Therefore, the temperature dependence of electrical resistivities of this ReO_4^{-} salt was measured along the conduction pathway (the *a* axis) using a two-terminal method. This salt indicated a room-temperature conductivity of 6×10^{-5} S cm^{-1} and showed semiconducting behavior from room temperature with an activation energy of $E_a = 0.16$ eV. Such a low conductivity and semiconducting behavior may originate from the weak intermolecular interaction between the radical cation states of dimers and the localized nature of spins that was cleared by Bonner−Fisher's fitting of magnetic susceptibilities.

CONCLUSION

In this paper, we reported the preparation, crystal structure analyses, and physical properties of new neutral and radical cation $Cu(hfac)_2$ complexes coordinated with TTF-1,3-benzothiazole hybrid ligands **1**. We cleared the unique molecular structures of the complexes in which two ligands are located parallelly in a transverse head-to-tail manner to each other and the $Cu(hfac)_2$ part was closely sandwiched by these two ligands. These complexes are insulators due to the lack of effective conduction pathways, but they clearly open the way for synthesis of new compounds using other metals and counteranions. On the other hand, we also cleared the structure and magnetic/conducting properties of the ReO_4^{-} salt of the unprecedented Cu^{I} complex in which two ligands **1** were connected to the central copper atom in a linear dicoordination. Two TTF parts of the neighboring complexes form a dimerized structure, and each TTF dimer in the radical cation state forms a one-dimensional uniform array along the *a* direction with a short S−S contact of 3.88 Å. Although the conducting property of this salt is not distinguished due to its weak intermolecular interaction between the dimers and the localized nature of conducting electrons, the unique $Cu(\mathbf{1})_2$-type molecular structure of the conducting moiety will create a series of new conducting materials in the near future. We are now engaged in preparation of other radical cation salts using the TTF—CH═CH—BTA ligands and several kinds of central transition metals to yield interesting conducting/magnetic bifunctional materials.

ASSOCIATED CONTENT

Supporting Information

X-ray crystallographic file for three crystals in CIF format, temperature dependence of $\chi_M T$ values of $Cu(hfac)_2(\mathbf{1})_2$ and $[Cu(hfac)_2(\mathbf{1})_2](AsF_6)_2$, electron paramagnetic resonance (EPR) spectra of $Cu(hfac)_2(\mathbf{1})_2$ and $[Cu(\mathbf{1})_2](ReO_4)_2$, and molecular orbital calculation of the $[Cu(\mathbf{1})_2]^{2+}$ part of $[Cu(\mathbf{1})_2](ReO_4)_2$. This material is available free of charge via the Internet at http://pubs.acs.org.

AUTHOR INFORMATION

Corresponding Author

*E-mail: hfuji@c.s.osakafu-u.ac.jp.

Notes

The authors declare no competing financial interest.

ACKNOWLEDGMENTS

This work was financially supported in part by Grants-in-Aid for Scientific Research (Nos. 20110006 and 21750150) from the Ministry of Education, Culture, Sports, Science and Technology of Japan and by a Grant from the Kansai Research Foundation for Technology Promotion. France-Japan GDRI (No. 91), University of Rennes 1, and Feder. We thank Mr. Kenji Iwase and Prof. Yuko Hosokoshi (Osaka Prefecture University) for measurement of EPR spectra.

REFERENCES

(1) In *TTF Chemistry: Fundamentals and Applications of Tetrathiafulvalene*; Yamada, J., Sugimoto, T., Eds.; Kodansha-Springer: Tokyo, 2004.
(2) Martín, N.; Sánchez, L.; Illescas, B.; Pérez, I. *Chem. Rev.* **1998**, *98*, 2527−2547.
(3) Metzger, R. M. *Acc. Chem. Res.* **1999**, *32*, 950−957.
(4) Bendikov, M.; Wudl, F.; Perepichka, D. F. *Chem. Rev.* **2004**, *104*, 4891−4945.
(5) Gorgues, A.; Hudhomme, P.; Sallé, M. *Chem. Rev.* **2004**, *104*, 5151−5184.
(6) Segura, J. L.; Martín, N. *Angew. Chem., Int. Ed. Engl.* **2001**, *40*, 1372−1409.
(7) D'Aléo, A.; Pointillart, F.; Ouahab, L.; Andraud, C.; Maury, O. *Coord. Chem. Rev.* **2012**, *256*, 1604−1620.
(8) Fujiwara, H.; Sugishima, Y.; Tsujimoto, K. *Tetrahedron Lett.* **2008**, *49*, 7200−7203.
(9) Tsujimoto, K.; Ogasawara, R.; Fujiwara, H. *Tetrahedron Lett.* **2013**, *54*, 1251−1255.
(10) Fujiwara, H.; Tsujimoto, K.; Sugishima, Y.; Takemoto, S.; Matsuzaka, H. *Physica B* **2010**, *405*, S12−S14.
(11) Furukawa, K.; Sugishima, Y.; Fujiwara, H.; Nakamura, T. *Chem. Lett.* **2011**, *40*, 292−294.
(12) Fujiwara, H.; Yokota, S.; Hayashi, S.; Takemoto, S.; Matsuzaka, H. *Physica B* **2010**, *405*, S15−S18.
(13) In *Handbook of Multifunctional Molecular Materials*; Ouahab, L., Ed.; Pan Stanford Publishing: Singapore, 2013.
(14) In *Conducting and Magnetic Organometallic Molecular Materials*; Fourmigué, M., Ouahab, L., Eds.; Springer-Verlag: Berlin, Heidelberg, 2009.
(15) Ouahab, L.; Enoki, T. *Eur. J. Inorg. Chem.* **2004**, 933−941.
(16) Coronado, E.; Day, P. *Chem. Rev.* **2004**, *104*, 5419−5448.
(17) Enoki, T.; Miyazaki, A. *Chem. Rev.* **2004**, *104*, 5449−5477.
(18) Ouahab, L. *Chem. Mater.* **1997**, *9*, 1909−1926.
(19) Kobayashi, H.; Cui, H.-B.; Kobayashi, A. *Chem. Rev.* **2004**, *104*, 5265−5288.
(20) Fujiwara, H.; Kobayashi, H. *Bull. Chem. Soc. Jpn.* **2005**, *78*, 1181−1196.
(21) Iwahori, F.; Golhen, S.; Ouahab, L.; Carlier, R.; Sutter, J.-P. *Inorg. Chem.* **2001**, *40*, 6541−6542. (b) Cosquer, G.; Pointillart, F.; Le Gal, Y.; Golhen, S.; Cador, O.; Ouahab, L. *Dalton Trans.* **2009**, 3495−3502.
(22) Setifi, F.; Ouahab, L.; Golhen, S.; Yoshida, Y.; Saito, G. *Inorg. Chem.* **2003**, *42*, 1791−1793.
(23) Zhu, Q.-Y.; Liu, Y.; Lu, W.; Zhang, Y.; Bian, G.-Q.; Niu, G.-Y.; Dai, J. *Inorg. Chem.* **2007**, *46*, 10065−10070.
(24) Chahma, M.; Hassan, N.; Alberola, A.; Stoeckli-Evans, H.; Pilkington, M. *Inorg. Chem.* **2007**, *46*, 3807−3809.
(25) Pointillart, F.; Cauchy, T.; Le Gal, Y.; Golhen, S.; Cador, O.; Ouahab, L. *Inorg. Chem.* **2010**, *49*, 1947−1960.
(26) Pointillart, F.; Golhen, S.; Cador, O.; Ouahab, L. *Dalton Trans.* **2013**, *42*, 1949−1960.
(27) Lorcy, D.; Bellec, N.; Fourmigué, M.; Avarvari, N. *Coord. Chem. Rev.* **2009**, *253*, 1398−1438.
(28) Caneschi, A.; Gatteschi, D.; Rey, P. *Progress in Inorganic Chemistry*; John Wiley & Sons: New York, 1991; Vol. *39*, pp 331−429.
(29) Benelli, C.; Gatteschi, D. *Chem. Rev.* **2002**, *102*, 2369−2387.
(30) Inoue, K.; Iwahori, F.; Markosyan, A. S.; Iwamura, H. *Coord. Chem. Rev.* **2000**, *198*, 219−229.
(31) Inoue, K. In *π-Electron Magnetism From Molecules to Magnetic Materials*; Veciana, J., Ed.; Springer-Verlag: Berlin, Heidelberg, New York, 2001; pp 61−91.
(32) Zahradnik, P.; Buffa, R. *Molecules* **2002**, *7*, 534−539.
(33) Dondoni, A.; Fantin, G.; Fogagnolo, M.; Medici, A.; Pedrini, P. *Tetrahedron* **1988**, *44*, 2021−2031.
(34) Garín, J.; Orduna, J.; Uriel, S.; Moore, A. J.; Bryce, M. R.; Wegener, S.; Yufit, D. S.; Howard, J. A. K. *Synthesis* **1994**, 489−493.
(35) Altomare, A.; Burlea, M. C.; Gamalli, M.; Cascarano, G. L.; Giacovazzo, C.; Guagliardi, A.; Polidre, G. *J. Appl. Crystallogr.* **1994**, *27*, 435.
(36) Beurskens, P. T.; Admiraal, G.; Beurskens, G.; Bosman, W. P.; de Gelder, D.; Israel, R.; Smith, J. M. M. *Technical Report of the Crystallography Laboratory*; University of Nijmegen: Nijmegen, The Netherlands, 1994.
(37) *CrystalStructure Analysis Package*; Molecular Structure Corp.: Houston, TX, 1992.
(38) König, E. *Landolt Bornstein, Group II: Atomic and Molecular Physics*; Springer-Verlag: Berlin, 1966; Vol. *2* (Magnetic Properties of Coordination and Organometallic Transition Metal Compounds).
(39) Guionneau, P.; Kepert, C. J.; Bravic, G.; Chasseau, D.; Truter, M. R.; Kurmoo, M.; Day, P. *Synth. Met.* **1997**, *86*, 1973−1974.
(40) Estes, W. E.; Gavel, D. P.; Hatfield, W. E.; Hodgson, D. *Inorg. Chem.* **1978**, *17*, 1415−1421.
(41) Frisch, M. J.; Trucks, G. W.; Schlegel, H. B.; Scuseria, G. E.; Robb, M. A.; Cheeseman, J. R.; Scalmani, G.; Barone, V.; Mennucci, B.; Petersson, G. A.; Nakatsuji, H.; Caricato, M.; Li, X.; Hratchian, H. P.; Izmaylov, A. F.; Bloino, J.; Zheng, G.; Sonnenberg, L.; Hada, M.; Ehara, M.; Toyota, K.; Fukuda, R.; Hasegawa, J.; Ishida, M.; Nakajima, T.; Honda, Y.; Kitao, O.; Nakai, H.; Vreven, T.; Montgomery, J. A., Jr.; Peralta, J. E.; Ogliaro, F.; Bearpark, M.; Heyd, J. J.; Brothers, E.; Kudin, K. N.; Staroverov, V. N.; Kobayashi, R.; Normand, J.; Raghavachari, K.; Rendell, A.; Burant, J. C.; Iyengar, S. S.; Tomasi, J.; Cossi, M.; Rega, N.; Millam, J. M.; Klene, M.; Knox, J. E.; Cross, J. B.; Bakken, V.; Adamo, C.; Jaramillo, J.; Gomperts, R.; Stratmann, R. E.; Yazyev, O.; Austin, A. J.; Cammi, R.; Pomelli, C.; Ochterski, J. W.; Martin, R. L.; Morokuma, K.; Zakrzewski, V. G.; Voth, G. A.; Salvador, P.; Dannenberg, J. J.; Dapprich, S.; Daniels, A. D.; Farkas, O.; Foresman, J. B.; Ortiz, J. V.; Cioslowski, J.; Fox, D. J. *Gaussian 09*, Revision A.1; Gaussian, Inc.: Wallingford, CT, 2009.
(42) Ichikawa, S.; Kimura, S.; Kazuyuki, T.; Mori, H.; Yoshida, G.; Manabe, Y.; Matsuda, M.; Tajima, H.; Yamaura, J. *Inorg. Chem.* **2008**, *47*, 4140−4145.
(43) Ichikawa, S.; Mori, H. *Inorg. Chem.* **2009**, *48*, 4643−4645.